Simulating Microbubble Flows Using COMSOL Multiphysics

Xiaodong(Sheldon) Chen[1], Samir N. Ghadiali[*1,2]
[1]Mechanical Engineering and Mechanics, Lehigh University, Bethlehem, PA 18015, [2]Bio Engineering program, Lehigh University, Bethlehem, PA 18015
*Corresponding author: Department of Biomedical Engineering, 270 Bevis Hall, 1080 Carmack Rd, Columbus OH 43210, ghadiali.1@osu.edu

Abstract: We utilized COMSOL with Matlab to develop a time dependent computational model of semi-infinite air bubble progression in a liquid filled channel. This microbubble flow model accounts simulates the continual interfacial expansion dynamics observed during the opening of collapsed pulmonary airways. We successfully simulated a wide range of capillary numbers (10^{-4} < Ca < 1) an at lower Ca than those used in our previous published boundary element models (BEM). Simulation results are compared to the low capillary asymptotic predictions of Bretherton, who found that the trailing film thickness varied as $Ca^{2/3}$ for $Ca < 2 * 10^{-3}$. Our COMSOL based model also accurately matched our previously published BEM results at $10^{-2} < Ca < 10^{1}$. This validated COMSOL model will be used in the future to simulate complex fluid-structure interactions between the microbubble and the soft tissue/biological cells surrounding the airway.

Keywords: Pulmonary airways; Acute respiratory distress syndrome (ARDS), Microbubble; Capillary number, Boundary Element Method (BEM); film thickness; asymptotic predictions; cellular deformation; shear and normal stress; finger width.

1. Introduction

Acute respiratory distress syndrome (ARDS) is a severe lung disease caused by a variety of direct and indirect insults. It is characterized by inflammation of the lung parenchyma leading to impaired gas exchange with concomitant systemic release of inflammatory mediators causing inflammation, hypoxemia and frequently resulting in multiple organ failure. The main treatment for ARDS is mechanical ventilation. The ventilation of fluid filled lungs involves the propagation of microbubbles over a layer of epithelial cells as shown in Figure 1. Unfortunately, experimental studies{1,2,6} have demonstrated that the large shear and normal stresses generated by microbubbles cause significant cellular deformation and injury. As a result, the mortality rates for ARDS remain high (~30-40%). The overall goal of our lab is to develop novel treatments for ARDS that minimize the amount of cellular deformation and injury caused by microbubble flows. However, experimental techniques are currently limited in their ability to monitor both the stresses generated by microbubbles and the cellular deformations caused by microbubbles. The goal of the current study is to develop computational models that accurately characterize the microbubble flows that exist during experimental conditions and to develop a model that can be extended in the future to simulate cell deformation during microbubble flows.

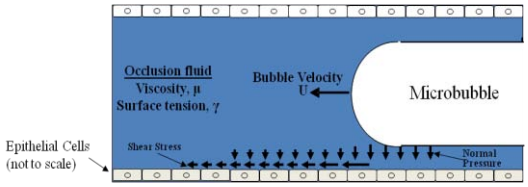

Figure 1: A schematic diagram of fluid stresses applied to epithelial cells during airway reopening.

Different computational techniques such as the Boundary Element Method (BEM) have been utilized by our lab in the past{3,4,5} to characterize the fluid mechanics of microbubble flows. However, the BEM has several limitations that do not allow for the simulation of experimental conditions. First, the BEM cannot simulate the very low capillary numbers ($Ca < 10^{-3}$) observed in the experiments. *Ca* is a dimensionless bubble velocity that represents the ratio of viscous to surface tension forces. At very low *Ca*, the microbubble lays down a very thin film of fluid and singularities associated with BEM cause numerical instabilities in this film. In addition, BEM is only valid for zero Reynolds number flows (i.e. Stokes flow) while experimental Reynolds numbers are O(1). Other investigators{7,8} have used the finite element method to obtain results at $10^{-4} < Ca < 10^{1}$,

and our goal is to used the COMSOL with MatLab software package to simulate very low *Ca* microbubble flows and to characterize the shear and normal stresses exerted by these flows.

2. Model Formulation

2.1 Governing Equations

In this paper, we used COMSOL to model one half of a semi-infinite bubble propagating in a rigid 2D channel. The incompressible Navier-Stokes fluid application mode is used to solve the problem. Starting with the momentum balance in terms of stresses, the generalized equation in terms of transport properties and velocity gradients are:

$$Re\frac{\partial U}{\partial t} - \nabla \cdot [Ca(\Delta U + (\Delta U)^T)] + Re(U \cdot \nabla)U + \nabla \mathrm{P} = F \quad (1)$$

$$\nabla \cdot \mathrm{U} = 0 \quad (2)$$

The first equation is the momentum transport equations, and the second is the equation of continuity for incompressible fluids. We are using dimensionless variables here, where Re is Reynolds number, $Re = \frac{\rho UD}{\mu}$, Ca is capillary number, $Ca = \frac{\mu U}{\gamma}$, P is the dimensionless pressure, $P = \frac{p}{\gamma/a}$, μ is the fluid kinematic viscosity, U is the bubble tip velocity at steady state, ρ is the density, γ is the surface tension, F is a volume force field such as gravity and a is the channel half-height. Our model incorporates a sub program written in MatLab which calculates the interfacial curvature in order to apply accurate boundary conditions at the air-liquid interface. The main force acting on the air-liquid interface is surface tension, which is directly related to the pressure drop according to Laplace's law:

$$\Delta P = P_{in} - P_{out} = \kappa \quad (3)$$

Here ΔP is the pressure drop across the interface, P_{in} is the pressure inside the microbubble, P_{out} is the outside fluid pressure, κ is the curvature of the interface. Our subprogram calculated the curvature using the following equations in Cartesian coordinates:

$$\kappa = \frac{\frac{dx}{ds}\frac{d^2y}{ds^2} - \frac{dy}{ds}\frac{d^2x}{ds^2}}{((\frac{dy}{ds})^2 + (\frac{dx}{ds})^2)^{3/2}} \quad (4)$$

$$n_x = -\frac{\frac{dy}{ds}}{((\frac{dy}{ds})^2 + (\frac{dx}{ds})^2)^{3/2}} \quad (5)$$

$$n_y = \frac{\frac{dx}{ds}}{((\frac{dy}{ds})^2 + (\frac{dx}{ds})^2)^{3/2}} \quad (6)$$

Where κ is the interface curvature, x and y are the coordinates, s is the arc-length of the interface, n_x is the normal vector in x direction and n_y is the normal vector in y direction. The current model can simulate a wide range of capillary numbers (i.e. $10^{-4} < Ca < 10^{1}$) and uses the ode113 MatLab routine to solve the interface equation of motion.

$$\frac{d\vec{Y}}{dt} = (\vec{u} \cdot \hat{n})\hat{n} \quad \text{where } \vec{Y} = x\hat{\imath} + y\hat{\jmath}, \vec{u} = u_x\hat{\imath} + u_y\hat{\jmath}, \hat{n} = n_x\hat{\imath} + n_y\hat{\jmath}. \quad (7)$$

2.2. Model Domain

The use of the COMSOL GUI environment allows for fast and simple post processing of the results. It is also easy and convenient to set up a problem and solve. However, we found that special subprograms must be implemented in the COMSOL with MATLAB environment to provide accurate boundary conditions and solutions.

A schematic of the fluid boundary and the location of the imposed boundary conditions in the lab frame are shown in figure 2. Table 1 defines the boundary condition for this problem and figure 3 shows a schematic finite element mesh. There are basically 3 types of boundary conditions. Boundary 1 is a parabolic flow profile with a flow rate that ensures a dimensionless tip velocity of 1 at steady-state. Boundary 3 and boundary 4 only have x direction constant velocity (i.e. no slip). Boundary 5 to 64 have an unknown velocity, so we define a curvature based stress boundary conditions on these surfaces. Figure 3 shows a schematic of the model with meshe at $Ca = 0.1$.

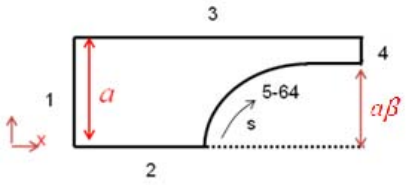

Figure 2: A schematic of the fluid boundary and the location of the imposed boundary conditions.

Boundaries	Boundary conditions
1	Parabolic flow, U=3aβ/2 $(y^2 - 1)$, v=0
2	symmetry
3	$u = 0$, v=0
4	$u = 0$, v=0
5-64	$\tau = \kappa \mathbf{n}$

Table 1: Description of boundary conditions

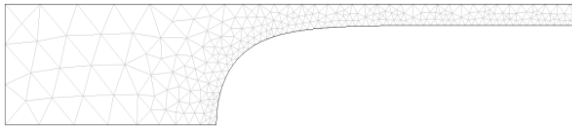

Figure 3: A schematic of the model with meshes at $\mathbf{Ca} = \mathbf{0.1}$.

3. Simulation Results

2.1 Convergence

For our simulations, we specify a relative error tolerance of $10^{-6}$and time steps of $\Delta t = 0.01$ in the ODE solver. The maximum normal velocity in the bubble-tip reference frame is used to check for steady-state convergence. Specifically, as the air liquid interface converges to a steady shape in the bubble fixed frame, the maximum normal velocity will tend to zero since in the bubble-tip reference frame the interface does not deform at steady-state. Figure 4 show the maximum normal velocity convergence plots for capillary numbers of 0.5 and 0.005. The convergence for the higher capillary number is smoother than the lower capillary number all solutions converge to maximum normal velocities less than 10^{-3}. Since the starting capillary for all the simulations is $Ca = 0.001$, it takes different time steps for the simulations to reach steady state at a given *Ca*.

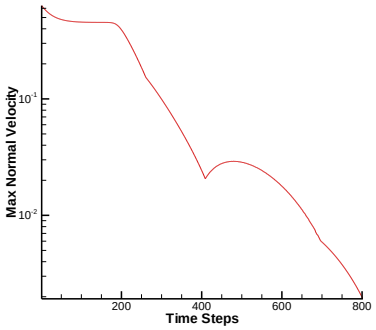

(a) $Ca = 0.5$

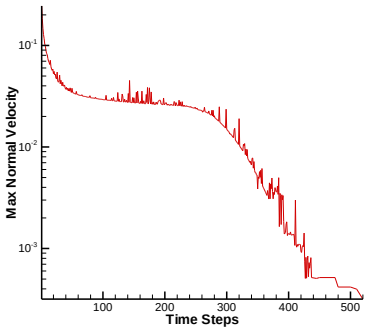

(b) $Ca = 0.005$

Figure 4: Convergence plots of due to the change of capillary numbers for (a) $Ca = 0.5$ and (b) $Ca = 0.005$ in the bubble fixed frame with $\Delta t = 0.01$.

Figure 5 demonstrate changes in the thin film thickness with respect to time. The starting capillary number is 0.001, the finger width for $Ca = 0.5$ will decrease because of the change of capillary, however, the finger width for $Ca = 0.0005$ will increase with the decreasing capillary.

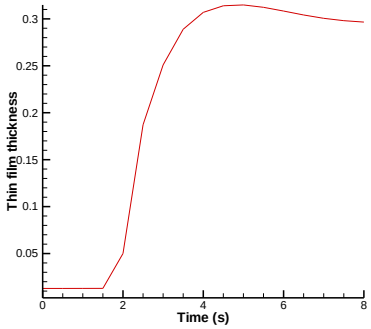

(a) $Ca = 0.5$

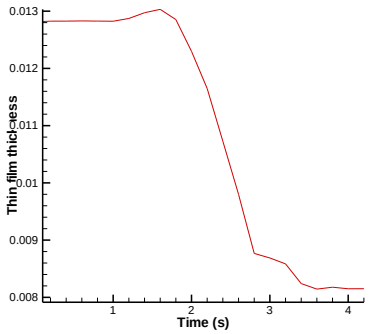

(b) $Ca = 0.0005$

Figure 5: Thin film thickness change due to the change of capillary numbers for (a) $Ca = 0.5$ and (b) $Ca = 0.0005$.

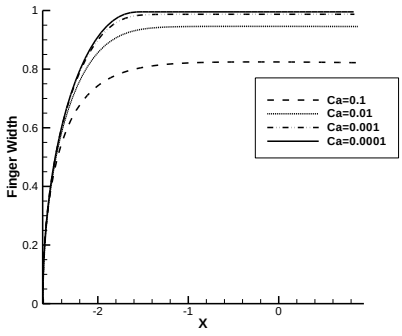

Figure 6: Interface change from the steady state for $Ca = 0.1$ to $Ca = 0.0001$ due to the flow rate change.

Figure 6 shows the air liquid interface change when Ca decreases from 0.1 to 0.0001. We can clearly find the thin film thickness decreases with the decreasing of the capillary number. When the capillary goes to 0.0001, the film thickness becomes very thin.

2.2 Other Results

Figure 7 shows the flow field surrounding the semi-infinite air bubble for a given capillary number as a function of time. The streamlines are drawn in the lab reference frame. In addition to flow visualization, this figure also shows how the interface shape and thin film thickness change with time.

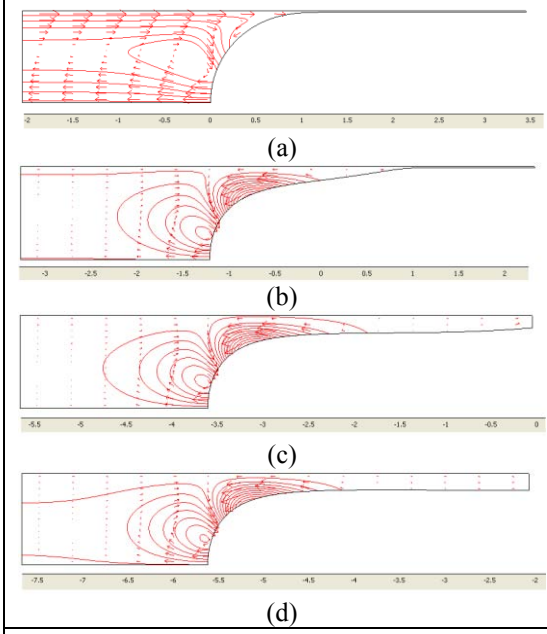

Figure 7: Diagram of the flow field surrounding the air liquid interface for $Ca = 0.1$ at different time steps (a) t=0, (b) t=1, (c) t=3 and (d) t=5, the streamlines are drawn in the lab frame.

4. Verification

In order to validate our FEM based simulations of microbubble flows, we compare our results with both an asymptotic analysis first performed by Bretherton {9} as well as previous results from our group obtained with the Boundary Element Method{4}.

For small Ca, Bretherton showed that

$$\delta \to 1.337Ca^{2/3} \; as \; Ca \to 0 \qquad (8)$$

where δ is thickness of the thin fluid film which trails the progressing air bubble. Here we first compare Bretherton's analytical predictions for δ with measurements of δ obtained with our COMSOL model. However, it is well known that the Bretherton's result, i.e. Eqn (8), is only valid in the limit of small Ca (i.e. $Ca < 2 * 10^{-3}$). Therefore, we also compare our COMSOL model with previous measurements of δ obtained in our lab with the Boundary Element Method (BEM). Since the BEM is only valid at very low Reynolds number we specify a Reynolds number of 10^{-5} in our COMSOL verification simulations. In addition, singularities in the BEM do not allow for accurate solutions at Ca < 10^{-2} and we therefore only make COMSOL – BEM comparisons at Ca > 10^{-2}.

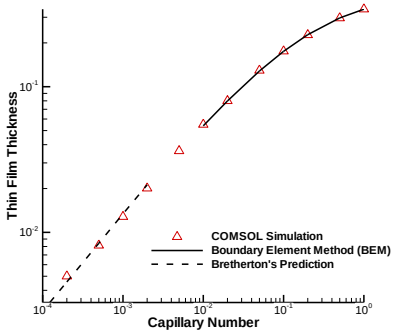

Figure 8: Comparison of the finger width with Bretherton's asymptotic predictions and Boundary Element Method data, x and y axis are in Log scale.

Figure 8 shows our COMSOL simulation results (filled triangles) for the film thickness, δ, from the lowest capillary number $Ca = 0.0001$ to the highest capillary number $Ca = 1$. As expected, the film thickness was found to decrease with decreasing Ca. In addition, the comparisons between our COMSOL simulations and Bretherton's predictions at low capillary numbers are all within 0.12% relative error while comparisons with the BEM solutions at higher capillary numbers are all within 0.15% relative error. We therefore conclude that our COMSOL simulations accurately match both analytical solutions and solutions obtained with other computational techniques.

5. Applications

Since we have verified these models through the comparison with other numerical methods, next we plan to use COMSOL with MatLab system to develop a fluid-structure interaction model that can accurately simulate cellular deformation during microbubble flows. As shown in Figure 1, there are epithelial cells on the channel wall during the bubble progression. There will be hydrodynamic stresses acting on epithelial cells, which will cause an imbalance of stresses along the cell, resulting in cell deformation and accordingly cell membrane injury during the airway opening. Through the analysis of the shear and normal stress, we could have a good understanding of the cell injury and cell death.

6. Conclusions

COMSOL with MATLAB provides a very flexible environment in which it is easy to implement specific subroutines written by our lab that accurately calculate interface curvature and movement. It was found to be capable of simulating two phase displacement in a channel for a wide range of capillary numbers much larger than our previous studies. Especially for those low capillary numbers that exist in the experiment. The lowest capillary number used here is $Ca = 0.0001$, but we are quite sure that we can still lower this number if needed. The simulation results are in excellent agreement with Bretherton's asymptotic predictions and Boundary Element Method, which validates our numerical method. As a result, we are able to obtain very accurate and stable solutions at very small capillary numbers compared to other methods during the simulation of the air liquid bubble interface movement. We plan to use these models to analyze experimental results and to extend this model in order to simulate cellular deformation and injury caused by microbubble flows.

8. References

1. Bilek AM, Dee KC, Gaver DP 3rd. Mechanisms of surface-tensioninduced epithelial cell damage in a model of pulmonary airway reopening. J Appl Physiol 94: 770–783, 2003

2. Kay SS, Bilek AM, Dee KC, Gaver DP 3rd. Pressure gradient, not exposure duration, determines the extent of epithelial cell damage in a model of pulmonary airway reopening. J Appl Physiol 97: 269–276, 2004

3. Ghadiali SN, Halpern D and Gaver DP 3rd, A Dual-Reciprocity Boundary Element Method for Evaluating Bulk Convective Transport of Surfactant in Free-Surface Flows. J Comput Phys 171: 534 –559, 2001

4. Ghadiali SN and Gaver DP 3rd, The influence of non-equilibrium surfactant dynamics on the flow of a semi-infinite bubble in a rigid cylindrical capillary tube. J. Fluid Mech. 478: 165–196, 2003

5. Dailey HL, Yalcin HC, Ghadiali SN, Fluid-structure modeling of flow-induced alveolar epithelial cell deformation. Comput & Struct 85: 1066-1071, 2007

6. Yalcin HC, Perry SF and Ghadiali SN, Influence of airway diameter and cell confluence on epithelial cell injury in an in vitro model of airway reopening. J Appl Physiol 103: 1796–1807, 2007

7. Giavedoni MD and Saita FA, The axisymmetric and plane cases of a gas phase steadily displacing a Newtonian liquid—A simultaneous solution of the governing equations. Phys. Fluids 9(8): 2420, 1997

8. Shen EI and Udell KS, A Finite Element study of low Reynolds number two-phase flow in cylindrical tubes. J. Appl. Mech. 52: 253, 1985

9. F.P.Bretherton. J. Fluid Mech. 10,166(1961)